AIAA JOURNAL
Vol. 33, No. 6, June 1995

New Approximation for Steady-State Response of General Damped Systems

A. E. Sepulveda*
University of California, Los Angeles, Los Angeles, California 90024
and
H. L. Thomas†
VMA Engineering, Colorado Springs, Colorado 80906

A new approximation for steady-state dynamic displacements, which captures the nonlinearities associated with resonance, is presented. This approximation is based on modal analysis and is valid for general damped structures, which include the case of actively controlled structures. Intermediate design variable and intermediate response quantity concepts are used to enhance the accuracy of the approximations. When these high-quality approximations are used within the context of the approximation concepts approach, the overall efficiency of the design synthesis process is improved by reducing the number of complete analyses required for convergence. Numerical results that illustrate the effectiveness of the method are presented.

Introduction

WHEN using the approximation concepts approach to structural synthesis, the number of design cycles needed for convergence is strongly dependent on the accuracy of the approximations used for the constrained structural responses. It is therefore desirable to use approximations that can accurately capture the nonlinear relationships between the structural responses and the actual design variables.

In the early stages of the development of the approximation concepts approach, approximate representations for constraints and objective functions were generated using first-order Taylor series expansions in terms of direct or reciprocal sizing type design variables.[1,2] More accurate approximations can be constructed, however, using approximations of intermediate response quantities, which were introduced in Ref. 2, in terms of selected intermediate design variables. The intermediate response quantity idea has been applied to static stress constraints,[3] frequency constraints,[4] steady-state undamped harmonic displacements,[5] control force constraints, complex eigenvalues,[6] and transient dynamic displacements.[7]

In this approach, simple approximations (e.g., linear, reciprocal, and hybrid) of intermediate response quantities (e.g., forces in the case of stress constraints and modal energies in the case of frequency constraints) in terms of selected intermediate design variables can be used while retaining the explicit nonlinear dependence of the constraints on the intermediate response quantities and the explicit relation between the intermediate design variables and the actual design variables.

Mathematically a constraint can be written as

$$g(R, x, y) \leq 0 \tag{1}$$

where $R_i, i \in I$, denotes the intermediate response quantities; $x_j, j \in J$, denotes the intermediate design variables; and $y_k, k = 1, \ldots, NDV$, are the actual design variables.

The following assumptions are made:

1) The term g is explicit in R_i, x_j, and y_k.

2) The various $R_i(x), i \in I$, are implicit functions of $x_j, j \in J$.

3) The various $x_j(y), j \in J$, are explicit functions of the actual design variables $y_k, k = 1, \ldots, NDV$.

Received April 5, 1994; revision received Aug. 2, 1994; accepted for publication Aug. 3, 1994.

*Assistant Professor, Mechanical, Aerospace, and Nuclear Engineering. Member AIAA.

†Senior Research and Development Engineer, 1767 South 8th St., Suite M-200. Member AIAA.

The approximations are constructed using Taylor series expansions of R_i in terms of x_j. For example, if a linear series is used,

$$\tilde{R}_i(x) = R_{i0} + \sum_{j \in J} \frac{\partial R_i(x_0)}{\partial x_j} (x_j - x_{j0}) \tag{2}$$

Substituting these approximations into Eq. (1), the approximation for g is then given by

$$\tilde{g}(y) = g(\tilde{R}(x(y)), x(y), y) \leq 0 \tag{3}$$

In the case of frequency response of damped structures, small changes in the design variables can lead to large changes in the dynamic response. This effect is particularly important near the resonance condition. In this paper, an approximation for the frequency response of general damped structures, which captures the nonlinearities associated with resonance, is introduced. This approximation is based on modal, rather than direct, solution of the frequency response and makes extensive use of the concepts of intermediate response quantities and intermediate design variables.

Dynamic Response

The general matrix equation of motion for a damped structure is given by

$$[M]\{\ddot{u}\} + [C]\{\dot{u}\} + ([K] + i[K_s])\{u\} = \{p\} \tag{4}$$

where $[M]$ is the mass matrix, $[C]$ is the viscous damping matrix, $[K]$ is the stiffness matrix, and $[K_S]$ represents the structural damping in the system. The matrices $[C]$ and $[K]$ will be considered nonsymmetric to include the case of actively controlled structures, $\{p\}$ is the vector of applied loads, and $\{u\}$ is the vector of dynamic displacements.

Modal Analysis

Defining the state-space variables as

$$\{q\} = \begin{Bmatrix} \dot{u} \\ u \end{Bmatrix} \tag{5}$$

Eq. (4) leads to the equations of motion in first-order form, namely,

$$[M^*]\{\dot{q}\} + [K^*]\{q\} = \{P\} \tag{6}$$

where

$$[M^*] = \begin{bmatrix} [0] & [M] \\ [M] & [C] \end{bmatrix} \tag{7a}$$

$$[K^*] = \begin{bmatrix} -[M] & [0] \\ [0] & [K] + i[K_S] \end{bmatrix} \tag{7b}$$

and

$$\{P\} = \begin{Bmatrix} \{0\} \\ \{p\} \end{Bmatrix} \tag{7c}$$

Let $\{\phi\}_r$ and $\{\chi\}_r$ denote the right and left complex eigenvectors (in the state space) associated with the right and left eigenproblems, respectively, i.e.,

$$(\lambda_r[M^*] + [K^*])\{\phi\}_r = \{0\} \qquad r = 1, \ldots, 2n \tag{8a}$$

$$\{\chi\}_r^T(\lambda_r[M^*] + [K^*]) = \{0\}^T \qquad r = 1, \ldots, 2n \tag{8b}$$

Clearly, for symmetric matrices $\{\phi\}_r = \{\chi\}_r$, $r = 1, \ldots, 2n$. In the previous equations n denotes the number of degrees of freedom of the system.

These eigenvectors can be partitioned into velocity and position components as

$$\{\phi\}_r = \begin{Bmatrix} \{\phi_v\} \\ \{\phi_p\} \end{Bmatrix}_r \tag{9a}$$

$$\{\chi\}_r = \begin{Bmatrix} \{\chi_v\} \\ \{\chi_p\} \end{Bmatrix}_r \tag{9b}$$

The velocity and position components are related such that[6]

$$\{\phi_v\}_r = \lambda_r\{\phi_p\}_r \tag{10a}$$

$$\{\chi_v\}_r = \lambda_r\{\chi_p\}_r \tag{10b}$$

The eigenvectors are normalized such that

$$\{\phi_p\}_r^T[M]\{\phi_p\}_r = 1 \tag{11a}$$

$$\{\chi\}_r^T[M^*]\{\phi\}_l = \delta_{rl} \tag{11b}$$

The complex eigenvalues λ_r appear in pairs of the form

$$\lambda_r^{(1)} = \sigma_r^{(1)} + i\omega_{dr} \tag{12a}$$

$$\lambda_r^{(2)} = \sigma_r^{(2)} - i\omega_{dr} \tag{12b}$$

The following particular cases are of interest.

Undamped case—$[C] = [0]$ and $[K_S] = [0]$:

$$\lambda_r^{(1)} = i\omega_r \tag{13a}$$

$$\lambda_r^{(2)} = -i\omega_r \tag{13b}$$

where ω_r is the rth natural frequency of the system.

Only viscous damping—$[K_S] = [0]$:

In this case the complex eigenvalues appear in complex conjugate pairs, i.e.,

$$\sigma_r^{(1)} = \sigma_r^{(2)} \tag{14}$$

Only structural damping—$[C] = [0]$:

$$\sigma_r^{(1)} = -\sigma_r^{(2)} \tag{15}$$

i.e., the pairs of eigenvalues are the negatives of each other.

In this paper a modal solution of the dynamic response problem will be used. In the modal solution approach it is assumed that the dynamic response can be represented by a truncated linear combination of complex mode shapes:

$$\{q\} = \sum_{r=1}^{2N} \{\phi\}_r \eta_r(t) \tag{16}$$

where N denotes the number of retained modes. The modes are ordered in ascending order of the damped frequencies, and the number N is determined depending on the forcing frequency.

Substituting Eq. (16) in Eq. (6) and premultiplying by $\{\chi\}_r^T$ leads to

$$T_r^*\dot{\eta}_r(t) + U_r^*\eta_r(t) = \{\chi\}_r^T\{P\} \tag{17}$$

where

$$T_r^* = \{\chi\}_r^T[M^*]\{\phi\}_r \tag{18a}$$

$$U_r^* = \{\chi\}_r^T[K^*]\{\phi\}_r \tag{18b}$$

and where from the definitions of T_r^* and U_r^* and Eq. (8a) premultiplied by $\{\chi\}_r^T$ it is easily seen that

$$\lambda_r = -\frac{U_r^*}{T_r^*} \tag{19}$$

and therefore Eq. (17) can be written as

$$\dot{\eta}_r(t) - \lambda_r\eta_r(t) = \frac{\{\chi\}_r^T\{P\}}{T_r^*} \tag{20}$$

Using the definitions of T_r^* and U_r^* given by Eqs. (18) and the relation between velocity and position parts of the eigenvectors [see Eqs. (10)], the following identities are obtained:

$$T_r^* = 2\lambda_r T_r + S_r \tag{21a}$$

$$U_r^* = -\lambda_r^2 T_r + U_r \tag{21b}$$

where T_r, U_r, and S_r are the modal energies (introduced in Ref. 6) given by

$$T_r = \{\chi_p\}_r^T[M]\{\phi_p\}_r \tag{22a}$$

$$U_r = \{\chi_p\}_r^T([K] + i[K_S])\{\phi_p\}_r \tag{22b}$$

and

$$S_r = \{\chi_p\}_r^T[C]\{\phi_p\}_r \tag{22c}$$

Also using the definition for P given in Eq. (7c),

$$\{\chi\}_r^T\{P\} = \{\chi_p\}_r^T\{p\} \tag{23}$$

Introducing Eqs. (21a) and (23) in to Eq. (20), the differential equations for the modal participation coefficients are then given by

$$\dot{\eta}_r(t) - \lambda_r\eta_r(t) = \frac{\{\chi_p\}_r^T\{p\}}{2\lambda_r T_r + S_r} \qquad r = 1, \ldots, 2n \tag{24}$$

For the steady-state case, the applied load can be written as

$$\{p\} = \{p_0\}e^{i\Omega t} \tag{25}$$

The solution of the system of equations given by Eq. (24) has the form

$$\eta_r(t) = A_r e^{i\Omega t} \tag{26}$$

where A_r denotes the amplitude for the participation coefficient η_r. Substituting Eqs. (25) and (26) into Eq. (24) gives

$$A_r = -\frac{(i\Omega + \lambda_r)\{\chi_p\}_r^T\{p_0\}}{(\Omega^2 + \lambda^2)(2\lambda_r T_r + S_r)} \tag{27}$$

Furthermore, the steady-state dynamic displacements are given by

$$\{u(t)\} = \{u_0\}e^{i\Omega t} \tag{28}$$

and the complex vector of amplitudes is given by

$$\{u_0\} = -\sum_{r=1}^{2N} \frac{(i\Omega + \lambda_r)\{\chi_p\}^T\{p_0\}}{(\Omega^2 + \lambda_r^2)(2\lambda_r T_r + S_r)}\{\phi_p\}_r \tag{29}$$

Undamped Case

If there is no damping in the system, considering the eigenvalue pairs as in Eq. (13), the dynamic response is given by

$$\{u_0\} = -\sum_{r=1}^{N}\left[\frac{(i\Omega + i\omega_r)}{(\Omega^2 - \omega_r^2)(2i\omega_r T_r)} + \frac{(i\Omega - i\omega_r)}{(\Omega^2 - \omega_r^2)(-2i\omega_r T_r)}\right] \times \{\phi_r\}^T\{p_0\}\{\phi_r\} \tag{30}$$

which can be written as

$$\{u_0\} = -\sum_{r=1}^{N} \frac{\{\phi_r\}^T\{p_0\}}{T_r(\Omega^2 - \omega_r^2)}\{\phi_r\} \tag{31}$$

This relation was obtained in Ref. 5. In this reference it was shown that for the case of undamped dynamic response a high-quality approximation could be generated by approximating the modal energies in Taylor series and then approximating the natural frequencies using a Rayleigh quotient approximation.

The linear Taylor series approximation with respect to the design variables x_i is given by

$$\tilde{T}_r = T_{r0} + \sum_{i=1}^{NDV} \frac{\partial T_r}{\partial x_i}(x_i - x_{i0}) \tag{32a}$$

$$\tilde{U}_r = U_{r0} + \sum_{i=1}^{NDV} \frac{\partial U_r}{\partial x_i}(x_i - x_{i0}) \tag{32b}$$

The partial derivatives used in the approximation are evaluated assuming that the mode shapes are invariant, i.e.,

$$\frac{\partial T_r}{\partial x_i} = \{\phi_r\}^T \frac{\partial[M]}{\partial x_i}\{\phi_r\} \tag{33a}$$

$$\frac{\partial U_r}{\partial x_i} = \{\phi_r\}^T \frac{\partial[K]}{\partial x_i}\{\phi_r\} \tag{33b}$$

The Rayleigh quotient approximation for the natural frequency is then given by

$$\tilde{\omega}_r^2 = \frac{\tilde{U}_r}{\tilde{T}_r} \tag{34}$$

from where the approximate displacement amplitude is given by

$$\{\tilde{u}_0\} = -\sum_{i=1}^{N} \frac{\{\phi_r\}^T\{p_0\}}{\tilde{T}_r(\Omega^2 - \tilde{\omega}_r^2)}\{\phi_r\} \tag{35}$$

Note that in Eq. (35) the natural mode shapes are assumed invariant, i.e., they are not approximated. The Rayleigh quotient, which appears in the denominator of Eq. (35), provides a high-quality approximation for the natural frequencies.[4] Thus, Eq. (35) captures the highly nonlinear behavior of the structural response near resonance, since if any of the retained structural frequencies is near the forcing frequency, the associated participation coefficient will be quite large if the normal mode shape is not orthogonal to the load vector.

Damped Response

The basic concepts introduced in Ref. 5 for the undamped case can be extended in a straightforward manner for the general damped case. For this case, the position parts of the right and left eigenvectors are assumed to be invariant. From this basic assumption a high-quality approximation for the complex eigenvalues can be generated by looking at the second-order eigenproblem (see Ref. 6),

$$\lambda_r^2 T_r + \lambda_r S_r + U_r = 0 \tag{36}$$

The complex modal energies T_r, S_r, and U_r are approximated in Taylor series, and the approximate eigenvalues $(\tilde{\lambda}_r)$ are obtained from

$$\tilde{\lambda}_r^2 \tilde{T}_r + \tilde{\lambda}_r \tilde{S}_r + \tilde{U}_r = 0 \tag{37}$$

The partial derivatives used in the approximation of T_r, S_r, and U_r are evaluated assuming that the position parts of the eigenvectors are invariant, i.e.,

$$\frac{\partial T_r}{\partial x_i} = \{\chi_p\}_r^T \frac{\partial[M]}{\partial x_i}\{\phi_p\}_r \tag{38a}$$

$$\frac{\partial U_r}{\partial x_i} = \{\chi_p\}_r^T \left\{\frac{\partial[K]}{\partial x_i} + i\frac{\partial[K_S]}{\partial x_i}\right\}\{\phi_p\}_r \tag{38b}$$

$$\frac{\partial S_r}{\partial x_i} = \{\chi_p\}_r^T \frac{\partial[C]}{\partial x_i}\{\phi_p\}_r \tag{38c}$$

Replacing the approximations for T_r, S_r, and U_r into Eq. (29), the approximate complex dynamic response is then given by

$$\{\tilde{u}_0\} = -\sum_{r=1}^{2N} \frac{(i\Omega + \tilde{\lambda}_r)\{\chi_p\}^T\{p_0\}}{(\Omega^2 + \tilde{\lambda}_r^2)(2\tilde{\lambda}_r\tilde{T}_r + \tilde{S}_r)}\{\phi_p\}_r \tag{39}$$

Note that this approximation reduces to the expression given in Eq. (31) when the system is undamped.

The error associated with this approximation comes from two assumptions. The first is that the displacements can be represented by a truncated set of modes (N). This is the error associated with the analysis and can be controlled by choosing a satisfactory value for N. The other assumption is that the position parts of the complex mode shapes are invariant with changes in the design variables. This error can be controlled by introducing appropriate move limits (ML) on the design variables at each design cycle. In the numerical examples of this paper it is shown that 70% move limits are not unreasonable.

Direct Solution or Full-Order Solution

In this section the direct solution of Eq. (4) will be reviewed to compare it with the approximations based on modal analysis introduced previously.

For the case of steady-state response, the solution to Eq. (4) is given by

$$\{u(t)\} = \{u_0\}e^{i\Omega t} \tag{40}$$

Replacing this expression in Eq. (4) gives a system of equations for the complex amplitude $\{u_0\}$,

$$[-\Omega^2[M] + i\Omega[C] + [K] + i[K_S]]\{u_0\} = \{p_0\} \tag{41}$$

where $\{p_0\}$ is the amplitude of the harmonic forcing function [see Eq. (25)].

Separating real and imaginary parts in $\{u_0\}$ as

$$\{u_0\} = \{u_0\}_R + i\{u_0\}_I \tag{42}$$

The complex system of equations given by Eq. (41) can be transformed into a real system of equations of dimension $2n$. In fact,

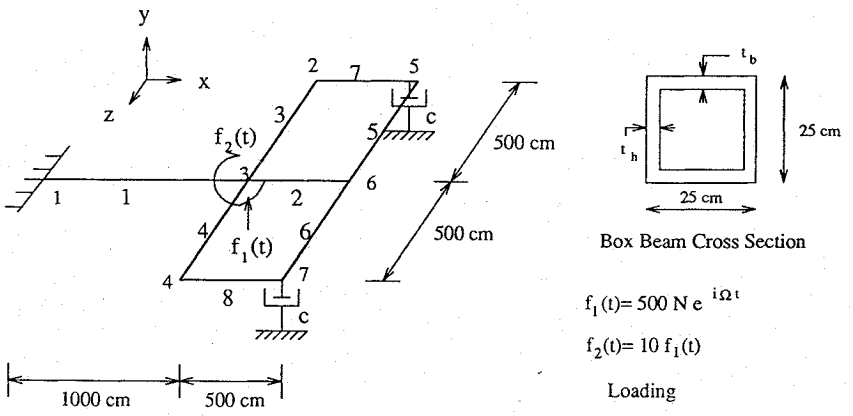

Fig. 1 Antenna structure.

introducing Eq. (42) into Eq. (41) and separating real and imaginary parts give

$$\begin{bmatrix} -\Omega^2[M]+[K] & -(\Omega[C]+[K_S]) \\ \Omega[C]+[K_S] & -\Omega^2[M]+[K] \end{bmatrix} \begin{Bmatrix} \{u_0\}_R \\ \{u_0\}_I \end{Bmatrix} = \begin{Bmatrix} \{P_0\} \\ \{0\} \end{Bmatrix} \tag{43}$$

This system can be solved for $\{u_0\}_R$ and $\{u_0\}_I$. These amplitudes are then approximated as direct, reciprocal, or hybrid[8] functions of the intermediate design variables or the actual design variables, so that

$$\{\tilde{u}_0\} = \{\tilde{u}_0\}_R + i\{\tilde{u}_0\}_I \tag{44}$$

The approximations given by Eq. (44) have two drawbacks. The first is that they are based on the direct solution of Eq. (4) [i.e., solution of Eq. (43)], which is very expensive for large problems. The second drawback is that they are poor approximations for the response whenever the loading frequency Ω is near a natural frequency of the structure because of the strong nonlinear effects of resonance, which cannot be captured by the approximations given by Eq. (44).

In the numerical examples, approximations based on the full-order solution will be used for comparison purposes to evaluate the accuracy of the new approximations based on the modal analysis presented in this paper.

Numerical Examples

The following examples show the effect of the proposed modal approximation in an optimization context. For the computational implementation, the approximate optimization problems were solved using DOT.[9] The convergence criterion for the example problems is the same one used in Ref. 6, i.e., the change in objective function is less than or equal to 0.1% for three consecutive iterations.

Problem 1—Antenna Structure

The first example involves the antenna structure shown in Fig. 1. The structure consists of eight aluminum beams ($E = 7.1 \times 10^6$ N/cm^2, $\rho = 2.77 \times 10^{-3}$ kg/cm^2, and $\nu = 0.325$) that have thin-walled hollow box beam cross sections (see Fig. 1). The structure is constrained to move vertically (y direction) only, and so each nodal point has 3 degrees of freedom (DOF) (y translation, and rotation about the x and z axes), resulting in the total of 18 DOF. Two dampers in the y direction are attached to nodes 5 and 7.

Structural elements are linked to produce a symmetric structure with respect to the x-y plane. Each beam element has two design variables (t_h and t_b, see Fig. 1) with initial design $t_h = t_b = 5$ cm, and side constraints are 0.5 cm $\leq t_h$, and $t_b \leq 10$ cm. The damping coefficients, which are also design variables, are also linked with an initial value of $c = 1N\cdot$ s/cm and side constraints such as $c \geq 0$ to preclude the possibility of unstable designs.

The structure is loaded at node 3 as shown in Fig. 1. Note that the loading will excite both bending and torsion in the structure.

Table 1 Initial complex eigenvalues, for antenna structure

Mode	Damping ratio,[a] %	Damped frequency, Hz
1	2.48	0.428
2	1.87	1.103
3	1.10	3.537
4	1.05	8.114
5	1.14	9.003

[a]Damping ratio: $\xi = -\sigma/\sqrt{\sigma^2+\omega_d^2}$.

Table 2 Final designs: Modal approximation for antenna structure—case 1

		Move limit, %		
Design element	Design variable	30	50	70
1	t_h	0.81	0.82	0.79
	t_b	1.05	1.03	1.05
2	t_h	0.67	0.71	0.94
	t_b	0.62	0.66	0.87
3	t_h	0.50	0.50	0.50
	t_b	0.50	0.50	0.50
4	t_h	8.38	8.43	8.31
	t_b	8.16	8.12	8.04
5	t_h	0.50	0.50	0.50
	t_b	0.50	0.50	0.50
Dampers	c	3.42	3.41	3.41
Weight, lb		2141	2144	2162
Number of analyses		13	13	9

The steady-state dynamic displacements at nodes 5 and 7 in the y direction are constrained to be less than 1 cm and the force in the dampers to be less than 15 N.

Case 1: $\Omega = 0.7$ Hz

In this first case the forcing frequency is chosen away from the resonance peaks (see Table 1). The iteration histories are plotted in Figs. 2 and 3 for both modal and full-order approximations for 30, 50, and 70% design variable move limits. The final designs are given in Tables 2 and 3. For all three move limits, both approximations converge to final designs within a range of 3% difference between final objective function values. From Figs. 2 and 3 it is observed that the modal approximation gives a much faster convergence, especially when 70% move limits are used. For all final designs the displacement constraints on nodes 5 and 7 and the force constraints for both dampers become critical.

Case 2: $\Omega = 0.5$ Hz

In this second case the forcing frequency is very near the first damped frequency of the initial design ($\omega_d = 0.43$ Hz). The iteration histories are plotted in Figs. 4 and 5 for both modal and full-order approximations for 30, 50, and 70% design variable move limits. In

Table 3 Final designs: full-order approximation for antenna structure—case 1

Design element	Design variable	Move limit, % 30	50	70
1	t_h	0.82	0.83	0.50
	t_b	1.05	1.05	0.50
2	t_h	0.50	0.50	0.50
	t_b	0.50	0.50	0.50
3	t_h	0.50	0.50	0.50
	t_b	0.50	0.50	0.50
4	t_h	8.40	8.58	9.99
	t_b	8.05	8.07	8.55
5	t_h	0.50	0.50	0.50
	t_b	0.50	0.50	0.50
Dampers	c	3.41	3.41	3.41
Weight, lb		2118	2129	2097
Number of analyses		18	18	25

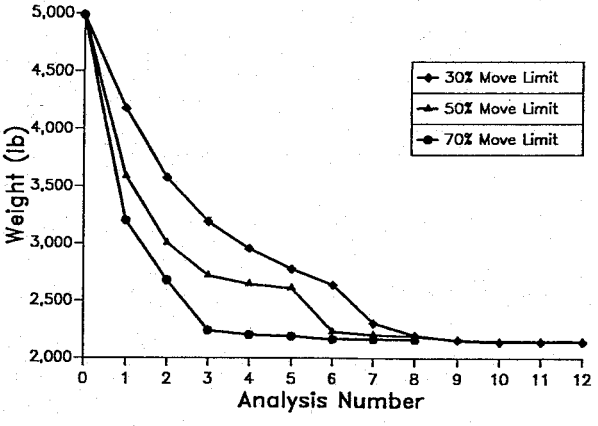

Fig. 2 Iteration histories, modal approximation, antenna structure—case 1.

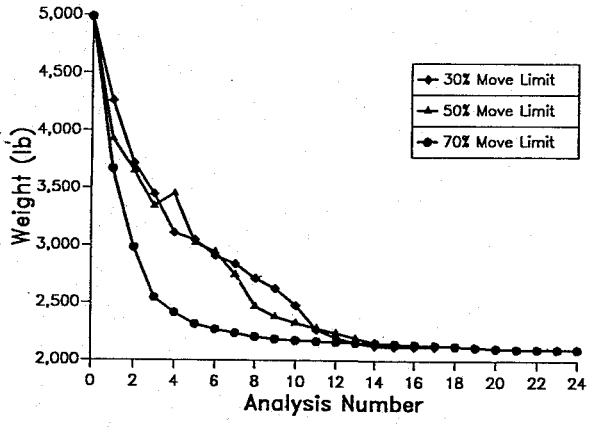

Fig. 3 Iteration histories, full-order approximation, antenna structure—case 1.

this case the full-order approximation fails to converge and oscillates, not being able to find a feasible design. The modal approximation converges in the 3 cases in less than 10 analyses. The final designs for these cases are given in Table 4. The critical constraints are the dynamic displacements on node 5 and the damper force at node 5.

It is interesting to observe that many of the member design variables achieve their upper bound, thus, producing a stiffer design, as compared with case 1, in which the first two modes are highly damped, leading to frequencies below the forcing frequency (ω_{d_1} = 0.15 Hz and ω_{d_2} = 0.28 Hz).

Table 4 Final designs: modal approximation for antenna structure—case 2

Design element	Design variable	Move limit, % 30	50	70
1	t_h	0.54	0.50	0.52
	t_b	0.50	0.50	0.50
2	t_h	10.0	10.0	10.0
	t_b	10.0	10.0	10.0
3	t_h	7.09	7.15	7.26
	t_b	6.73	6.75	6.72
4	t_h	10.0	10.0	10.0
	t_b	10.0	10.0	10.0
5	t_h	10.0	10.0	10.0
	t_b	10.0	10.0	10.0
Dampers	c	4.76	4.77	4.74
Weight, lb		5681	5681	5684
Number of analyses		10	8	9

Table 5 Final design response ratios for problem 2—grillage structure

Constraint	Response ratio Ref. 6	New results
Displacement (joint 1)	0.996	0.982
Displacement (joint 6)	0.996	0.897
Displacement (joint 19)	1.000[a]	1.000[a]
Displacement (joint 24)	1.000[a]	0.988
Stability (mode 1)	−4.630	−2.991
Stability (mode 2)	−5.121	0.628
Stability (mode 3)	0.763	0.600
Stability (mode 4)	0.959	1.000[a]
Actuator force (joint 8)	0.332	0.321
Actuator force (joint 11)	0.332	0.295
Actuator force (joint 14)	0.463	0.216
Actuator force (joint 17)	0.463	0.220
Total control force	1.000[a]	0.628

[a]Constraint is critical.

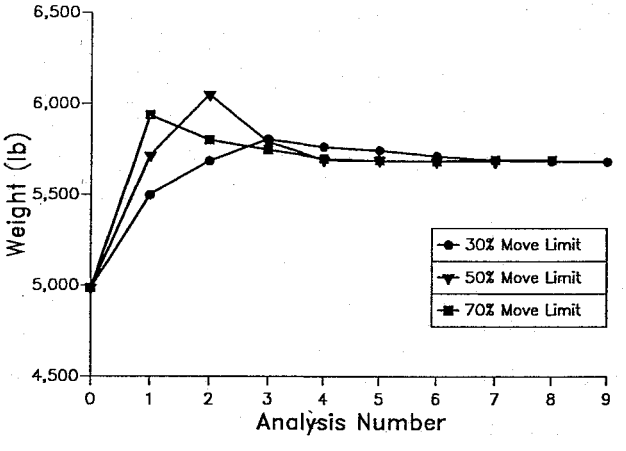

Fig. 4 Iteration histories, modal approximation, antenna structure—case 2.

Problem 2—Grillage

This example is taken from Ref. 6 and consists of the design synthesis of the 4 × 6 (72 DOF) controlled grillage structure shown in Fig. 6. The grillage consists of 10 aluminum frame members (ρ = 0.1 lb/in.^{3}, $E = 10.5 \times 10^6$ lb/in.^{2}, and $\nu = 0.3$) placed on 2-ft centers and cantilevered from two fixed supports by 2-ft-long flexible beams. Each solid rectangular beam is 2.0 in. wide and has an initial thickness of 0.25 in. The frame element member thicknesses along with the thickness of the cantilevered supports (elements 39 and 40) make up 11 structural design variables. The members are oriented so that the width dimension lies in the plane of the structure. There

Table 6 Control system final design for problem 2—grillage structure

		Actuator joint							
		Ref. 6				New results			
Sensor joint	Design variables	8	11	14	17	8	11	14	17
8	h_p	−0.002	—	—	—	0.001	—	—	—
	h_v	0.000	—	—	—	0.005	—	—	—
11	h_p	—	−0.002	—	—	—	0.000	—	—
	h_v	—	0.000	—	—	—	0.005	—	—
14	h_p	—	—	−0.009	—	—	—	0.001	—
	h_v	—	—	0.000	—	—	—	0.003	—
17	h_p	—	—	—	0.009	—	—	—	0.001
	h_v	—	—	—	0.000	—	—	—	0.003
1	h_p	−0.003	−0.003	0.005	0.006	−0.003	−0.004	0.001	0.001
	h_v	0.022	0.005	−0.016	−0.019	0.006	0.004	0.002	0.000
6	h_p	−0.003	−0.003	0.006	0.005	0.001	0.000	0.001	0.001
	h_v	0.005	−0.022	−0.019	−0.016	0.005	0.005	0.003	0.003
19	h_p	−0.002	−0.002	0.005	0.006	−0.004	−0.003	0.001	0.001
	h_v	0.000	0.000	0.000	0.000	0.005	0.004	−0.001	0.002
24	h_p	−0.002	−0.002	0.006	0.005	−0.002	−0.002	0.000	0.000
	h_v	0.000	0.000	0.000	0.000	0.002	0.002	0.005	0.005

Table 7 Structural final design for problem 3—grillage structure

	Thickness, in.	
Beam numbers	Ref. 6	New results
1–5	0.274	0.323
6–10	0.100[a]	0.100[a]
11–15	0.100[a]	0.100[a]
16–20	0.197	0.165
21–23	0.100[a]	0.100[a]
24–26	0.132	0.163
27–29	0.100[a]	0.100[a]
30–32	0.100[a]	0.100[a]
33–35	0.132	0.154
36–38	0.100[a]	0.100[a]
39–40	0.442	0.367

[a]At lower bound.

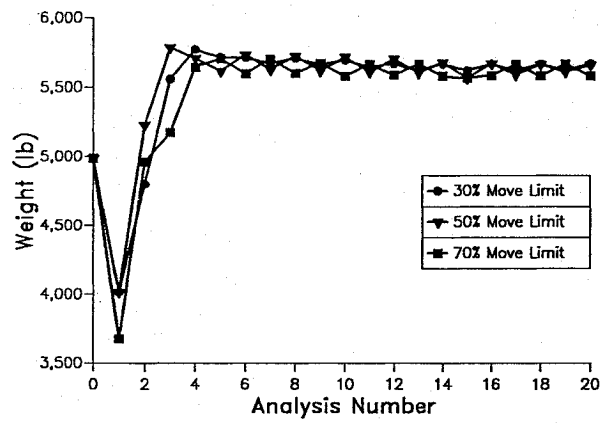

Fig. 5 Iteration histories, full-order approximation, antenna structure—case 2.

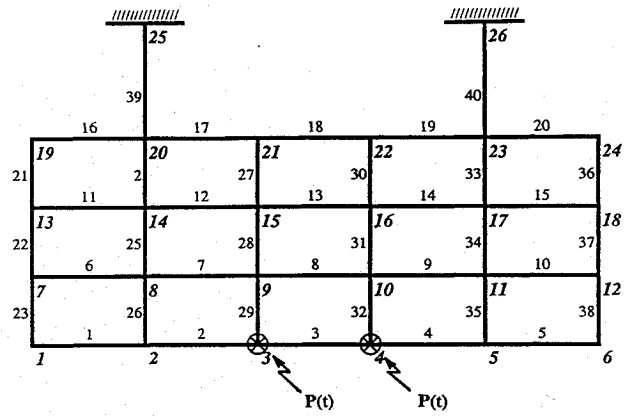

Fig. 6 Grillage structure.

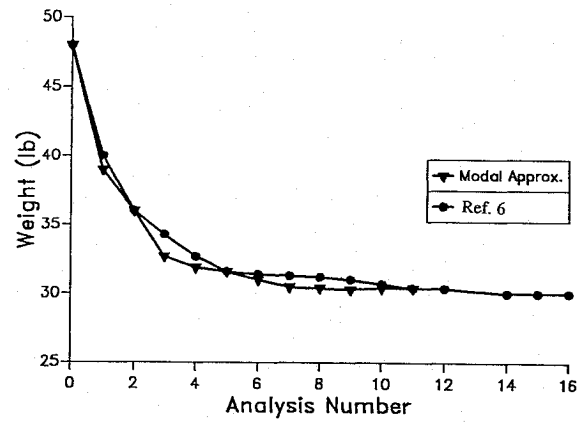

Fig. 7 Iteration histories, grillage structure.

are actuators attached to the structure at joints 8, 11, 14, and 17 that act in the z direction. The mass of each actuator (0.5 lbm) is modeled as a fixed nonstructural mass. Sensors, which sense position and velocity in the z direction, are located at joints 1, 6, 19, and 24, as well as 8, 11, 14, and 17. Each actuator is connected to the four corner sensors (at joints 1, 6, 19, and 24) and the sensor at the same joint as the actuator. This results in five sensors per actuator and a total of 40 gain design variables. The initial gains are h_p = 0.0001 lb/in., and h_v = 0.0001 lb-s/in. This problem has 51 design variables, 2% structural damping is assumed.

The structure is subjected to 5.0 lb loads at 2 Hz at joints 3 and 4 in the z direction. The amplitudes of the dynamic displacements of the corner of the grillage (joints 1, 6, 19, and 24) are constrained to be less than or equal to 2.0 in. The magnitude of each actuator force is constrained to be less than or equal to 2.0 lb. The real part of the complex eigenvalues is constrained to be below −0.05 rad/s for mode 1, −0.10 rad/s for mode 2, −0.20 rad/s for mode 3, and −0.20 rad/s for mode 4. Finally, the total control force is constrained to be less than or equal to 3.15 lb. In this problem, 80% move limits were used during each design stage.

The iteration history data are plotted in Fig. 7. The final design response ratios, final design control system variable values, and final design structural variable values are presented in Tables 5–7. The final weight using the modal approximations is 30.4 lb, which is 1.2% higher than the final weight obtained in Ref. 6 (30.03 lb). But the convergence is obtained in 12 instead of 17 analyses. It is important to note that in Ref. 6 high-quality approximations are used

for the complex eigenvalues, and a full-order approximation using intermediate design variables is used for the dynamic displacements.

Conclusions

It has been shown that the modal approximation for dynamic displacements significantly improves convergence characteristics when applied to problems with frequency response constraints. Moreover, the modal approximation is quite accurate even when the design is near resonance and large move limits are used.

In constructing explicit approximations for dynamic response constraints, the flexibility of intermediate response quantities and intermediate design variables has been extensively exploited. It should be recognized that the choice of the intermediate design variables depends on the type of structural element used in the design process. Herein, the cross-sectional properties A, I_1, I_2, and J were employed as the intermediate structural design variables. In this work the intermediate response quantities U_n, T_n, and S_n (modal energies) were approximated linearly in terms of the intermediate design variables, but a hybrid expansion can be used if more conservative approximations are required.

Finally, the inherent disjointness of design spaces that occurs. when constraints are placed on dynamic displacements, observed in Ref. 10 and explained in Ref. 11, is captured by the modal approximation. The approximations presented here make it possible to attack this difficulty by using heuristic methods (e.g., Refs. 12 and 13) or by applying some kind of global optimizer to solve the approximate problem (e.g., see Ref. 14).

References

[1]Schmit, L. A., and Farshi, B., "Some Approximation Concepts for Efficient Structural Synthesis," *AIAA Journal*, Vol. 12, No. 5, 1974, pp. 692–699.

[2]Schmit, L. A., and Miura, H., "Approximation Concepts for Efficient Structural Synthesis," NASA CR 2552, March 1976.

[3]Vanderplaats, G. N., and Salajegheh, E., "A New Approximation Method for Stress Constraints in Structural Synthesis," *AIAA Journal*, Vol. 27, No. 3, 1989, pp. 352–358.

[4]Canfield, R. A., "An Approximation Function for Frequency Constrained Structural Optimization," *AIAA Journal*, Vol. 28, No. 6, 1990, pp. 1116–1122.

[5]Thomas, H. L., Sepulveda, A. E., and Schmit, L. A., "Improved Approximations for Dynamic Displacements Using Intermediate Response Quantities," *Proceedings of the Third NASA/Air Force Symposium on Recent Advances in Multidisciplinary Analysis and Optimization* (San Francisco, CA), Sept. 1990, pp. 95–104.

[6]Thomas, H. L., Sepulveda, A. E., and Schmit, L. A., "Improved Approximations for Control Augmented Structural Optimization," *AIAA Journal*, Vol. 30, No. 1, 1992, pp. 171–179.

[7]Sepulveda, A. E., Thomas, H. L., and Schmit, L. A., "Improved Transient Response Approximations for Control Augmented Structural Optimization," *Proceedings of the Second Pan American Congress of Applied Mechanics*, UTFSM, Valparaiso, Chile, 1991, pp. 611–614.

[8]Lust, R. V., and Schmit, L. A., "Control-Augmented Structural Synthesis," *AIAA Journal*, Vol. 26, No. 1, 1988, pp. 86–94.

[9]Vanderplaats, G. N., DOT Users Manual, Version 4.00, VMA Engineering, Colorado Springs, CO 80906, 1993.

[10]Cassis, J. H., "Optimum Design of Structures Subjected to Dynamic Loads," Univ. of California, Los Angeles, UCLA-ENG-7451, School of Engineering and Applied Science, Los Angeles, CA, June 1974.

[11]Johnson, E. H., "Disjoint Design Spaces in the Optimization of Harmonically Excited Structures," *AIAA Journal*, Vol. 14, No. 2, 1976, pp. 259–261.

[12]Mills-Curran, W. C., and Schmit, L. A., "Structural Optimization with Dynamic Behavior Constraints," *AIAA Journal*, Vol. 23, No. 1, 1985, pp. 131–138.

[13]Miura, H., and Chargin, M., "Automated Tuning of Airframe Vibration by Structural Optimization" *Proceedings of the 42nd Annual Forum and Display*, The American Helicopter Society, Washington, DC, 1986, pp. 111–120.

[14]Sepulveda, A. E., and Schmit, L. A., "Approximation Based Global Optimization Strategy for Structural Synthesis," *AIAA Journal*, Vol. 31, No. 1, 1993, pp. 180–188.